

# Carbon Nanofiber Electrodes and Controlled Nanogaps for Scanning Electrochemical Microscopy Experiments

Ran Tel-Vered, Darren A. Walsh,<sup>†</sup> Masoud A. Mehrgardi,<sup>‡</sup> and Allen J. Bard\*

Department of Chemistry and Biochemistry and the Center for Nano and Molecular Science, The University of Texas at Austin, Austin, Texas 78712

The electrochemical behavior of electrodes made by sealing carbon nanofibers in glass or with electrophoretic paint has been studied by scanning electrochemical microscopy (SECM). Because of their small electroactive surface area, conical geometry with a low aspect ratio and high overpotential for proton and oxygen reduction, carbon nanofiber (CNF) electrodes are promising candidates for producing electrode nanogaps, imaging with high spatial resolution and for the electrodeposition of single metal nanoparticles (e.g., Pt, Pd) for studies as electrocatalysts. By using the feedback mode of the SECM, a CNF tip can produce a gap that is smaller than 20 nm from a platinum disk. Similarly, the SECM used in a tip-collection substrate-generation mode, which subsequently shows a feedback interaction at short distances, makes it possible to detect a single CNF by another CNF and then to form a nanometer gap between the two electrodes. This approach was used to image vertically aligned CNF arrays. This method is useful in the detection in a homogeneous solution of short-lifetime intermediates, which can be electrochemically generated at one electrode and collected at the second at distances that are equivalent to a nanosecond time scale.

A nanogap is an electrode arrangement in which two collinear electrodes are separated by a gap of nanometer dimensions. There have been a number of studies involving nanogaps, most of these involving studies of the electronic transport properties of single molecules, which bridge the gap (e.g., DNA or other macromolecules).<sup>1,2</sup> Nanogaps are usually prepared with fixed dimensions, e.g., by mechanically produced break junctions,<sup>3</sup> break junctions formed by electromigration,<sup>4</sup> electrodeposition,<sup>5</sup> carbon nanotube extracted lithography,<sup>6</sup> direct e-beam lithography,<sup>7</sup> and

conventional microscale fabrication techniques such as optical lithography, electron-beam evaporation, and liftoff.<sup>8</sup> In most cases, the exact gap dimensions are uncontrolled, although there have been reports of the formation of controlled nanogaps of fixed dimensions by several different approaches.<sup>9–11</sup> Our group has been interested in nanogaps whose dimensions are continuously variable, for example, in connection with studies of single-molecule electrochemistry<sup>12</sup> and in studies of rapid homogeneous reactions coupled to electron-transfer reactions at electrodes.<sup>13</sup>

Generally, kinetic studies of electrochemically generated, unstable species can be achieved if the species lifetime is of the order of the diffusion time across the gap,  $d^2/2D$ , where  $d$  is the gap separation and  $D$  is the diffusion coefficient. To increase the range of systems that can be studied by scanning electrochemical microscopy (SECM) to chemical species with lifetimes in the microsecond and nanosecond region, one must develop experimental strategies for decreasing  $d$  to the nanometer level, i.e., to a nanogap. This can be achieved by using extremely small probes (UMEs) that can approach a substrate or another electrode to very small distances. With glass-insulated disk electrodes, of the type most frequently used in SECM, one is limited by the RG value of the electrode, i.e., the ratio of the radius of glass insulating shroud to that of the metallic disk electrode. Another problem associated with disk UMEs is that the exposed electroactive part is sometimes recessed slightly beneath the insulating layer. While this has only a minor effect during micrometer-scale measurements, any feedback-based approach to a nanometer distance often results in the insulator touching the substrate and blocking any further movement of the recessed electroactive disk. A useful approach to solving this problem is to use conical electrodes that can approach the substrate or another similar electrode to very small  $d$  values without colliding.

Conical UMEs have been previously studied by a combination of scanning electron microscopy (SEM), steady-state voltammetry,

\* To whom correspondence should be addressed: ajbard@mail.utexas.edu.  
<sup>†</sup> Present address: School of Natural Sciences, Chemistry, University of Newcastle upon Tyne, Newcastle upon Tyne NE1 7RU, UK.  
<sup>‡</sup> Present address: Chemistry Department, Institute for Advanced Studies in Basic Sciences, Zanjan 45195, Iran.  
(1) Porath, D.; Bezryadin, A.; de Vries, S.; Dekker, C. *Nature* **2000**, *403*, 635.  
(2) Xu, B.; Zhang, P.; Li, X.; Tao, N. *Nano Lett.* **2004**, *4*, 1105.  
(3) Reed, M. A.; Zhou, C.; Mueller, C. J.; Burgin, T. P.; Tour, J. M. *Science* **1997**, *278*, 252.  
(4) Park, H.; Lim, A. K. L.; Park, J.; Alivisatos, A. P.; McEuen, P. L. *Appl. Phys. Lett.* **1999**, *75*, 301.  
(5) Morpurgo, A. F.; Marcus, C. M.; Robinson, D. B. *Appl. Phys. Lett.* **1999**, *74* (14), 2084.

(6) Chung, J.; Lee, K.-H.; Lee, J. *Nano Lett.* **2003**, *3* (8), 1029.  
(7) Hu, W.; Bernstein, G. H.; Sarveswaran, K.; Lieberman, M. *Proc. IEEE-Nano*, **2003**.  
(8) Choi, J.; Lee, K.; Janes, D. B. *Nano Lett.* **2004**, *4* (9), 1699.  
(9) Chen, F.; Qing, Q.; Ren, L.; Wu, Z.; Liu, Z. *Appl. Phys. Lett.* **2005**, *86*, 123105/1.  
(10) Strachan, D. R.; Smith, D. E.; Johnston, D. E.; Park, T.-H.; Therien, M. J.; Bonnell, D. A.; Johnson, A. T. *Appl. Phys. Lett.* **2005**, *86*, 043109/1.  
(11) He, H. X.; Boussaad, S.; Xu, B. Q.; Li, C. Z.; Tao, N. J. *J. Electroanal. Chem.* **2002**, *522*, 167.  
(12) Bard, A. J.; Fan, F.-R. F. *Acc. Chem. Res.* **1996**, *29*, 572.  
(13) Bi, S.; Liu, B.; Fan, F.-R. F.; Bard, A. J. *J. Am. Chem. Soc.* **2005**, *127*, 3690.

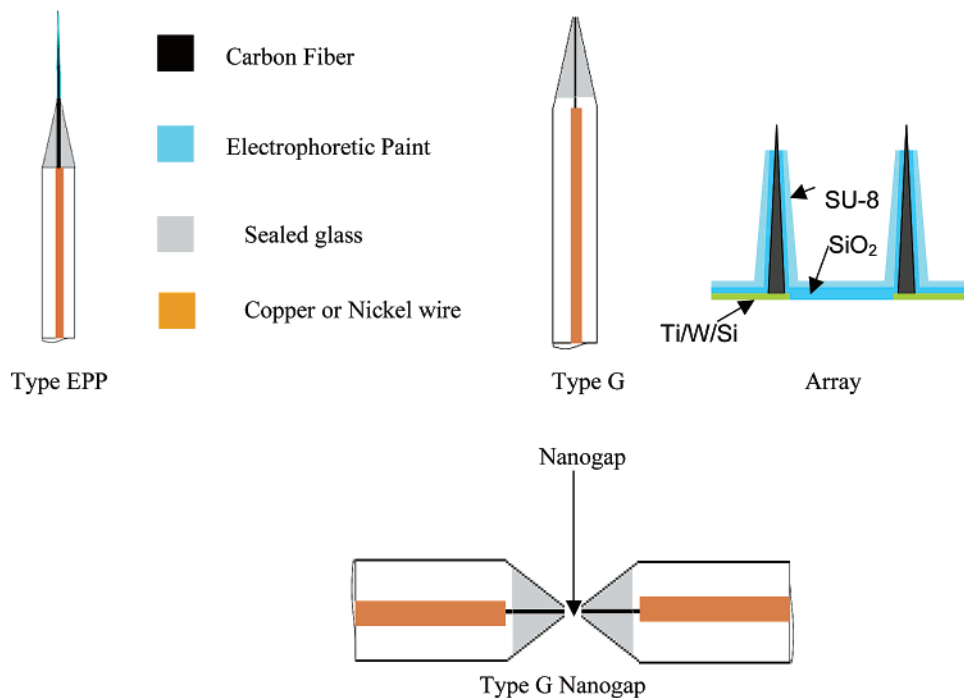


**Figure 1.** Schematic diagram of tips and nanogaps.

and SECM.<sup>14–17</sup> Our choice to work with carbon nanofiber (CNF) conical electrodes was due to three main advantages: (1) carbon fibers can be easily flame-etched to a final radius of curvature of 50–250 nm; (2) after insulation, e.g., with anodic electrophoretic paint, the exposed CNF shows a reasonably low aspect ratio (2.0), which is fairly sensitive to feedback;<sup>18</sup> (3) carbon electrodes show high overpotentials to proton and oxygen reduction and therefore the CNFs can be employed over a wider useful range of potentials in aqueous solutions compared to Pt.

We are also particularly interested in using nanogaps, rather than simply an approach of a nanometer electrode to a large substrate, in experiments to study electrocatalytic reactions at single metal nanoparticles. It is possible to nucleate a single nanoparticle at a UME, as was shown in some of the earliest SECM experiments.<sup>19–22</sup> In the nanogap configuration, it should then be possible to generate an electroactive species such as oxygen at the bare ultramicroelectrode tip, which will then diffuse to the microelectrode-supported nanoparticle where it can be electroreduced. This type of experiment has recently been described for supported catalysts although the catalyst particle size was not controlled.<sup>23</sup> The use of two microscopic electrodes rather than a single UME and large, planar surface to form a nanogap has the advantage of allowing one to easily locate the

nanoparticle under investigation, which can be difficult when locating single particles on a large planar surface using SECM or scanning tunneling microscopy. As discussed in this paper, we are also interested in using nanogaps to study homogeneous kinetics of reactions associated with electron-transfer reactions. A nanogap with a very small separation is easier to form, since the interference by the insulator of the electrode touching the surface before the tip is within the desired distance is less of a problem. In this paper, we describe the construction of the CNF electrodes and their characterization. We show how these can be used to form adjustable nanogaps and describe briefly their application to the examination of vertically aligned CNF arrays (VACNF arrays)<sup>24</sup> and kinetic measurements.

## EXPERIMENTAL SECTION

**Materials.** All chemicals were reagent grade and were used as received. All solutions were prepared with deionized water (Milli-Q, Millipore Corp.). Carbon yarn (10  $\mu\text{m}$  in diameter) was from Strem Chemicals (Newburyport, MA). Anodic electrophoretic paint (Glassphor ZQ 84-3225) was from BASF (Münster, Germany) and diluted 1:20 with water prior to use. Silver epoxy was from Epoxy Technology (Billerica, MA). Chips containing arrays of VACNFs located within a microfluidic channel were prepared by Dr. T. E. McKnight and co-workers using micro-fabrication techniques as described previously.<sup>24</sup>

**CNF Electrode Preparation.** Two different types of CNF tips were used: type EPP, low aspect ratio conical tips with electrophoretic paint insulation for use in aqueous solutions, and type G, carbon disks sealed in glass, which can also be used in nonaqueous solvents (Figure 1). Type EPP CNF tips used in these studies were prepared using similar flame etching<sup>25</sup> and insulation techniques<sup>26,27</sup> to those previously reported.

(14) Treutler, T. H.; Wittstock, G. *Electrochim. Acta* **2003**, *48*, 2923.

(15) Macpherson, J. V.; Unwin, P. R. *Anal. Chem.* **2000**, *72*, 276.

(16) Shao, Y.; Mirkin, M. V.; Fish, G.; Kokotov, S.; Palanker, D.; Lewis, A. *Anal. Chem.* **1997**, *69*, 1627.

(17) Mirkin, M. V.; Fan, F.-R. F.; Bard, A. J. *J. Electroanal. Chem.* **1992**, *328*, 47.

(18) Zoski, C. G.; Liu, B.; Bard, A. J. *Anal. Chem.* **2004**, *76*, 3646.

(19) Hills, G.; Pour, A. K.; Scharifker, B. *Electrochim. Acta* **1983**, *28*, 891.

(20) Scharifker, B.; Hills, G. *J. Electroanal. Chem.* **1981**, *130*, 81.

(21) Budevski, E.; Bostanov, V.; Vitanov, T.; Stoyanov, S.; Kotzawa, A.; Kaischew, R. *Electrochim. Acta* **1966**, *11*, 1697.

(22) Markov, I.; Toshev, S. *Electrodeposition Surf. Treat.* **1975**, *3*, 385.

(23) Fernandez, J. L.; Walsh, D. A.; Bard, A. J. *J. Am. Chem. Soc.* **2005**, *127*, 357.

(24) McKnight, T. E.; Melechko, A. V.; Austin, D. W.; Sims, T.; Guillorn, M. A.; Simpson, M. L. *J. Phys. Chem. B* **2004**, *108*, 7115.

(25) Maus, R. G.; Wightman, R. M. *Anal. Chem.* **2001**, *73*, 3993.

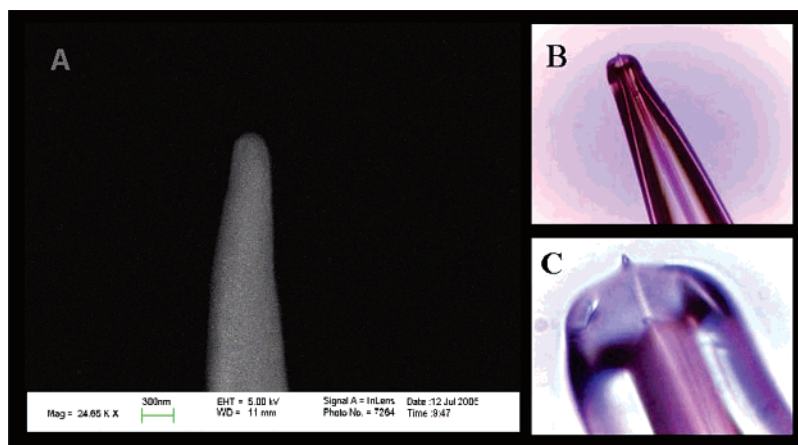


**Figure 2.** (A) SEM image of a CNF after insulation with electrophoretic paint. The beam energy was 5.00 kV and the focal distance was 11 mm. (B, C) Optical micrographs of a CNF protruding from a borosilicate capillary. Optical lenses used were  $\times 5$  and  $\times 50$  for (B) and (C), respectively.

**Type EPP Electrodes.** Glass pipets were prepared from borosilicate tubes (o.d. 1.2 mm, i.d. 0.69 mm) using a laser pipet puller (model P-2000, Sutter Instrument Co., Novato, CA), yielding micropipet tips with inner diameters of  $\sim 20 \mu\text{m}$  and tapers that were  $\sim 0.5 \text{ cm}$  in length. Approximately 1 cm of  $10\text{-}\mu\text{m}$ -diameter CNF was attached to one end of a piece of Ni–Cr (Nichrome) wire using a small amount of silver epoxy and cured in an oven for 45 min at  $100 \text{ }^\circ\text{C}$ . The wire/CNF assembly was then inserted into the top of the pulled micropipet and pushed through so that  $\sim 3 \text{ mm}$  of the CNF protruded from the micropipet tip. Epoxy cement was injected into the top of the capillary to attach the Ni–Cr wire to the glass tube and hold the CNF rigid. The glass at the tip was then sealed around the CNF using a cool low-oxygen natural gas flame, by inserting the pipet tip into the flame for  $\sim 0.5 \text{ s}$ . The part of the CNF that protruded from the glass pipet was then flame-etched in an oxygen-rich (bright blue) flame to a length of  $50 \mu\text{m}$  or less using periodic observation by optical microscopy to monitor the progress of etching. During this step, it was very important to etch the CNF alone, without melting the glass seal. This was done by a very slow manual insertion of the CNF into the flame. An orange glow from the CNF indicated that etching was proceeding. Typically, three flame etches were performed, each lasting  $\sim 1 \text{ s}$ .

The etched carbon fiber was insulated with anodic electrophoretic paint. It was immersed into a 1:20 solution of the paint in water, and a Pt coil surrounding the CNF was the reference/auxiliary electrode. A dc potential of 2.2 V was applied to the CNF for 40 s, after which time, the oxidation current had decreased to a small steady value of 0.2–1.0 nA. The electrode assembly was then heated at  $150 \text{ }^\circ\text{C}$  for 3 min. This process has been shown to slightly shrink the deposited paint film, exposing the tip.<sup>28</sup> The entire deposition and heating process was repeated once to ensure good insulation of the sides of the CNF.

**Type G Electrodes.** A piece of CNF was inserted in a 10-cm-long, nominal 1-mm-i.d. borosilicate tube sealed at one end. The open end of the tube was connected to the vacuum line and heated

within a Ni–Cr wire coil for  $\sim 30 \text{ min}$  to desorb any impurities or moisture on the wire and glass tube. One end of the CNF was then sealed in the glass at the closed end of the tube by increasing the heating coil temperature. Electrical connection to the unsealed end of the wire was made with silver epoxy to a copper wire. The glass wall surrounding the conducting disk was sharpened with emery paper (grit 600) and  $6\text{-}\mu\text{m}$  diamond paste, while frequently examining it with an optical microscope until an RG  $\sim 2\text{--}3$  was obtained.

**Electrochemical Experiments.** A CH Instruments model CHI 900B (CH Instruments, Austin, TX) was employed for electrochemical measurements.

**VACNF Arrays.** An array chip of vertically aligned CNF electrodes was used as the substrate and a type EPP electrode was used as the working electrode. An electrochemical cell was constructed on the VACNF chip by attaching a small piece of hollow glass tubing (height 1 cm, diameter 1 cm) to the chip using an epoxy resin, forming a watertight seal on the chip surface. A silver quasi-reference electrode (Ag QRE) and Pt counter electrode were used for all measurements.

**Dual-Type EPP CNF Nanogap Formation.** A type EPP tip was mounted inside a hollow Teflon cylinder that was wrapped with Teflon tape. The tip was inserted using mild force and positioned pointing upward in a 5-mL cylindrical Teflon SECM cell with a hole in its bottom. In this way, the stationary substrate electrode was tightly held vertically pointing upward, and no leakage of electrolyte from the cell could be detected. A second type EPP tip was brought parallel to the substrate electrode using the piezoelements of the SECM. The electrochemical alignment of the two tips was preceded by positioning the two tips  $\sim 1 \text{ mm}$  apart using the piezocontrol. About 4 mL of electrolyte was added to the cell, ensuring that both electrode tips were immersed in solution. Further experimental details are given in the Results and Discussion section.

## RESULTS AND DISCUSSION

**Characterization of CNF Electrodes. Optical Methods.** Several different electrochemical and optical methods were used to characterize these electrodes. SEM yields information about the geometry, radius, and shape of the flame-etched CNF. The CNF tip in Figure 2A shows a typical hemispherical apex with a radius

(26) Walsh, D. A.; Fernández, J. L.; Mauzeroll, J.; Bard, A. J. *Anal. Chem.* **2005**, *77*, 5182.

(27) Lee, A.; Bard, A. J. *Anal. Chem.* **2002**, *74*, 3626.

(28) Slevin, C. J.; Gray, N. J.; Macpherson, J. V.; Webb, M. A.; Unwin, P. R. *Electrochem. Commun.* **1999**, *1*, 282.

of curvature of nearly 150 nm. Generally, the range of radii observed for many tips was 50–250 nm depending on variations in the etching time, flame temperature, and exact position of the tip in the flame. Further verification that only the CNF was protruding from the center of the glass capillary without molten glass is demonstrated by the optical micrographs in Figure 2B,C. Neither SEM nor optical microscopy can resolve the thin carbonaceous electrophoretic polymer insulation layer on the carbon fiber. The voltammograms in Figure 3A show that the thin paint coating caused a significant capacitance, much larger than that expected from just the exposed tip. The charging current was linear with the sweep rate ( $v$ ) and was especially pronounced at the highest  $v$ . The specific capacitance calculated from the slope of the current versus sweep rate curve was 3 orders of magnitude higher than expected ( $\sim 10 \mu\text{F cm}^{-2}$ , for carbon), suggesting that the contribution of the capacitance extends to the carbon fiber several micrometers beyond the exposed part beneath the very thin electrophoretic paint layer.

**Voltammetry in Solution.** Besides evaluation of the CNF tip by optical methods to obtain an estimate of the radius of curvature,  $r_{\text{vis}}$ , one can electrochemically determine the tip radius by cyclic voltammetry at a slow scan rate in the presence of a redox mediator. If a hemispherical apex geometry (which is in a good agreement with Figure 2A) is assumed, the electrochemically evaluated radius,  $a$ , can be evaluated according to

$$a = i_{\text{ss}} / 2\pi nFD_0C_0 \quad (2)$$

where  $D_0$  is the diffusion coefficient of the mediator species,  $C_0$  is the mediator concentration, and  $i_{\text{ss}}$  is the steady-state diffusion limiting current (in our study  $i_{\text{ss}}$  was measured at  $E = 350 \text{ mV}$  vs Ag/AgCl for a 1 mM ferrocenemethanol (FcMeOH) mediator).

A systematic comparison between  $r_{\text{vis}}$  and  $a$  revealed good agreement, within less than 10%. This finding suggests that most of the electroactive area is located at the very end of the apex and that the contribution by pinholes in the electrophoretic insulating paint to the total faradaic current is negligible. Furthermore, while SEM cannot distinguish between the CNF and the carbonaceous electrophoretic paint, the good correlation between the radii is useful in evaluating the aspect ratio ( $H$ ) at the CNF apex. A closer look at Figure 2A shows a radius of curvature that is nearly 150 nm. Since the tip starts to broaden right from its apex, this geometry will only hold for aspect ratios that are  $\sim 0.5$  or less. From a SECM experimental point of view, this means that the exposed part of the CNF is blunt, approaching a disk-shaped geometry, so it is expected to maintain high sensitivity to feedback currents.

**Approach Curves at Air/Solution Interface.** To probe the quality of the electrophoretic paint deposition and for the existence of possible pinholes, the CNF electrodes were tested with SECM by translating the insulated tip from air into a solution containing FcMeOH, a technique that has been described in detail previously.<sup>26,27</sup> The CNF tip was positioned in air  $\sim 500 \mu\text{m}$  above a FcMeOH solution surface and was held at 0.35 V versus Ag/AgCl where a diffusion-limited FcMeOH oxidation current occurs when the tip is inside the solution. The tip was then moved slowly (200 nm/s) toward the solution, until initial contact between the exposed carbon apex and the electrolyte was achieved, as

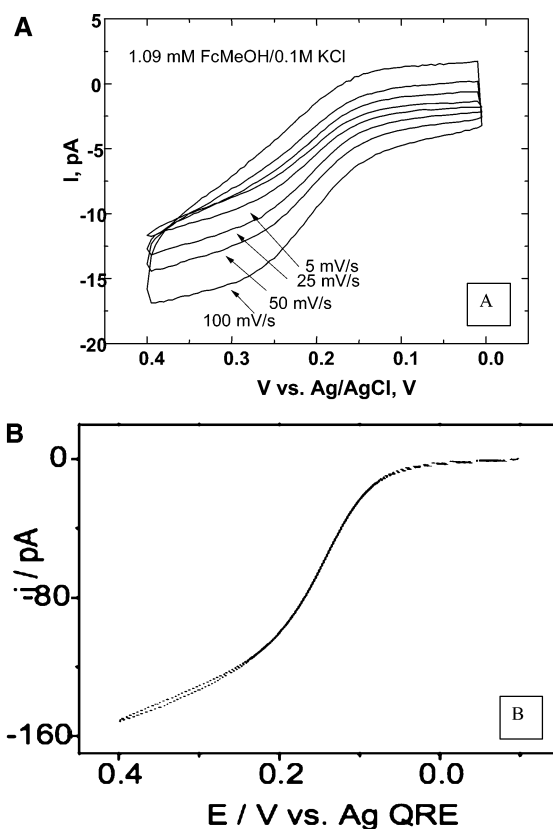


**Figure 3.** (A) Cyclic voltammograms for a 150-nm-radius CNF tip in 1.09 mM FcMeOH/0.1 M KCl electrolyte at various sweep rates. (B) Cyclic voltammogram for a 400-nm-radius insulated CNF electrode in 1 mM FcMeOH/0.1 M KCl. The potential limits are  $-0.1$  to  $0.4 \text{ V}$ , and the initial potential was  $-0.1 \text{ V}$ . The potential sweep rate was  $50 \text{ mV/s}$ .

indicated by a current jump caused by the appearance of both faradaic and charging current. The tip was further moved into the solution and the current monitored until no increase could be detected. Evidence of a good insulating layer is a single current increase as the tip enters the solution and FcMeOH begins to be oxidized at the CNF surface. A poor insulating film shows a series of current spikes as the tip is immersed deeper into the solution; these are attributed to pinholes in the electrophoretic paint layer. Although the probability of finding pinholes decreased sharply when shorter (a few micrometers in length) CNFs were used, and in most cases no holes were detected even at very slow scans, electrodeposition experiments have shown that a pinhole-free electrode is hard to obtain.

**Approach Curves in Solution.** Although the above methods can give a useful indication of tip size and quality, they are less useful at determining the detailed geometry at the tip apex, e.g., whether the tip is slightly recessed into the insulation. For this purpose, SECM approach curves over conductive and insulation substrates are useful.<sup>18</sup> When the conductive tip is recessed, such an approach will show almost no change in the current until it crashes at the substrate surface. Such approach curves must be carried out with careful alignment of the tip and substrate and with a very slow approach to avoid crashing the tip, which inevitably destroys it. For example, for a tip with  $a = 50 \text{ nm}$ , one will not see significant deviations from  $i_{T,\infty}$  before the separation distance,  $d$ , is  $\sim 200 \text{ nm}$ . For an approach speed of  $50 \text{ nm/s}$  (which is still



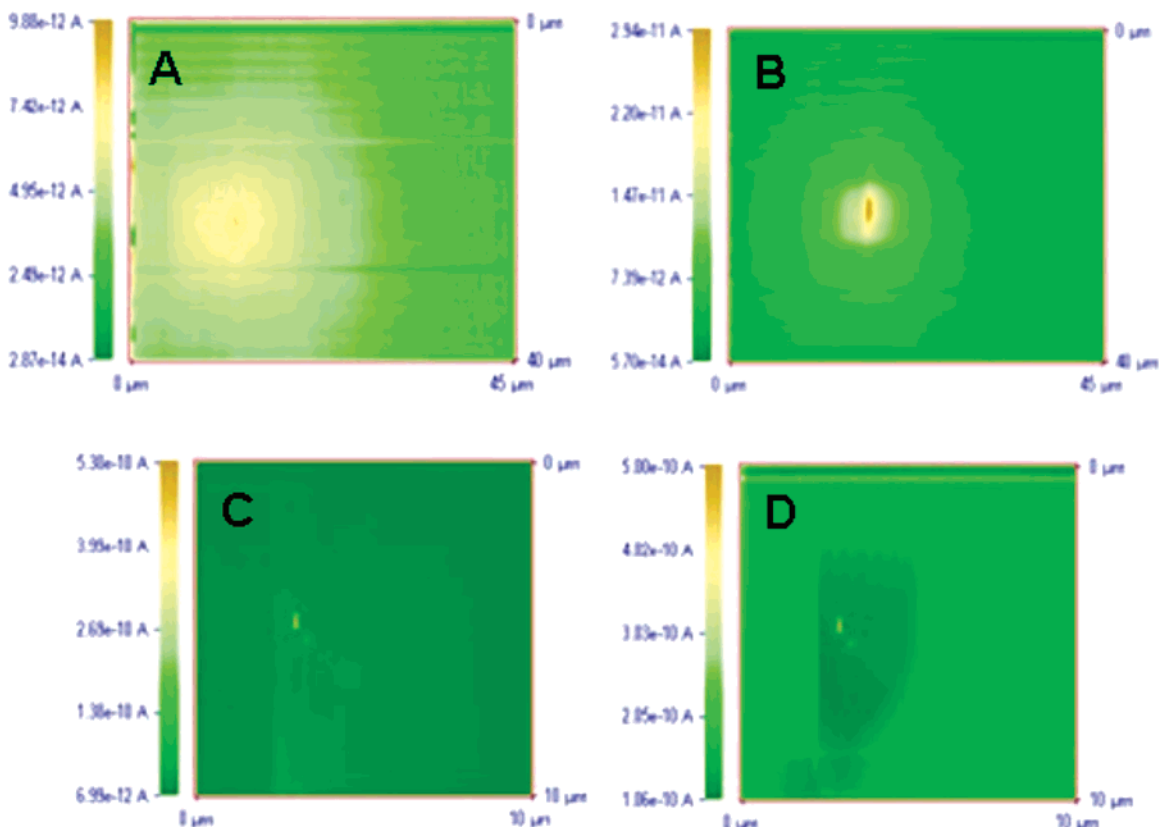


**Figure 4.** Dual CNF tips electrochemical recognition experiment. SECM is operated in SG-TC of  $\text{FcMeOH}^+$ . The electrolyte is 1.02 mM  $\text{FcMeOH}$  in 0.1 M  $\text{KCl}$ . The probe tip had  $r = 250$  nm and was held at  $E_{\text{probe}} = 0.00$  V vs  $\text{Ag}/\text{AgCl}$ . The substrate had  $r = 220$  nm and was held at  $E_{\text{sub}} = 0.35$  V vs  $\text{Ag}/\text{AgCl}$ . (A–C) demonstrate the substrate images as shown by the probe tip current over a scanned  $xy$  area, followed by gradually decreasing the electrode gap in the  $z$  direction (images are  $5 \mu\text{m}$  apart). (D) is the mirror image of (C) and represents the probe tip image as measured by feedback at the substrate.

rather large to get a good approach curve) and visually setting the tip  $\sim 200 \mu\text{m}$  above the substrate, it takes well over 1 h to get to the distance where an approach curve registers changes because of feedback. Thus, the approach curves we obtained with type EPP tips were not completely satisfactory (Supporting Information, Figure S1). Figure S1A shows the theoretical (solid line)<sup>18</sup> and experimental feedback approach curve obtained for a larger (400 nm) CNF tip upon approaching an insulating surface. The best fit obtained was for a cone with a radius,  $a = 0.4 \mu\text{m}$ ,  $H$  (aspect ratio) = 2, and an RG (ratio of insulator radius to radius of the cone at base) = 1.2. Figure S1B presents a slow (50 nm/s) approach curve of a 150-nm-diameter CNF tip over a platinum disk electrode. As can be seen, no feedback current was observed until a nanometer gap of  $\sim 10$  nm has been formed between the electrodes. Further approach of the tip to decrease the nanogap size resulted in a sharp enhancement in the feedback current and finally led to an electrode crash. Also presented in Figure S1B are theoretical approach curves calculated for a disk UME and for cone UME with a low aspect ratio ( $H = 0.1$ ).<sup>18</sup> Compared to the experimental CNF behavior, the theoretical curves exhibit enhanced feedback current at much larger tip–substrate distances. However, in the nanogap region, the feedback current of the CNF seems to increase more rapidly than the  $H = 0.1$  cone UME. One possible explanation for this effect is that a contribution of tunneling current starts to become significant when the two electrodes are biased. Alternatively, this may indicate that the

theoretical model used for the approach curve does not account for forces that become significant at very short ( $< 10$  nm) distances.

**Nanogap Experiments.** *Dual CNF Electrochemical Spatial Recognition.* Formation of the nanogap requires alignment of the two electrodes so that the electroactive portions overlap in the  $xy$  plane followed by control of the  $z$  distance to form the gap. Consider the experiment where a CNF tip is inserted face up to a center hole at a bottom of Teflon cell. The upper (probe) tip is connected to the piezoelement of the SECM, which controls its spatial  $xyz$  position whereas the bottom (substrate) electrode is stationary. Because the electrodes are relatively far apart initially, feedback current is not significant. Instead, the initial approach must be made using the substrate-generation/tip-collection (SG-TC) SECM mode. Since the tip will collect material produced at the substrate over distances that largely depend on the substrate electrolysis time, i.e., within the growing substrate diffusion layer, it will sense the presence of the substrate at distances where feedback effects are very small. In this mode, 1 mM  $\text{FcMeOH}$  in 0.1 M  $\text{KCl}$  was introduced into the cell covering both CNF tips. The substrate was held at  $E_{\text{subs}} = 0.35$  V versus  $\text{Ag}/\text{AgCl}$  to obtain a steady  $\text{FcMeOH}$  to  $\text{FcMeOH}^+$  oxidation current. This was done concurrently with the probe tip set to  $E_{\text{probe}} = 0.0$  V versus  $\text{Ag}/\text{AgCl}$ , where reduction of any  $\text{FcMeOH}^+$  diffusing to the vicinity of the electrode occurred. When this anodic current was detected, the probe tip was scanned in the  $xy$  plane so that the position of

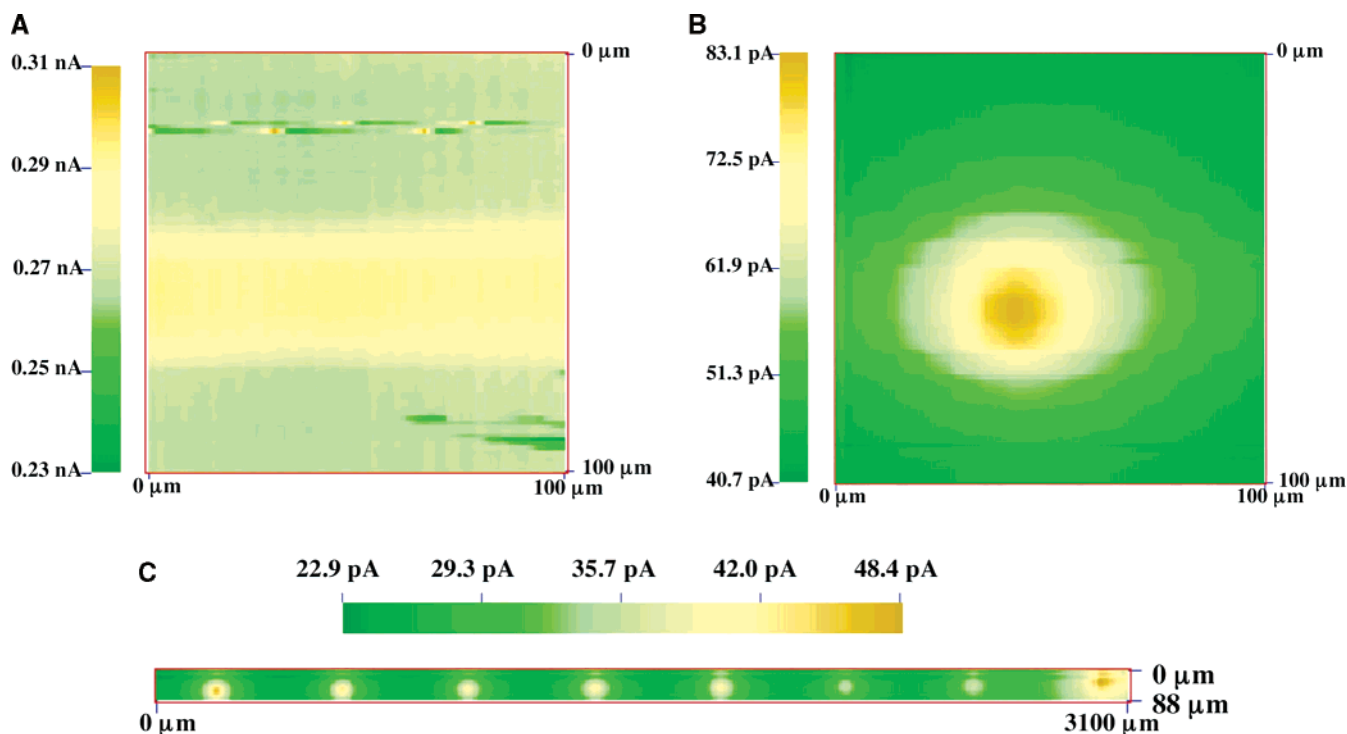


**Figure 5.** (A) SECM image obtained upon scanning the tip over a 100- $\mu\text{m}^2$  portion of the chip surface in 1 mM FcMeOH/0.1 M KCl. The tip potential was 0.4 V and the substrate was at open circuit potential. (B) SECM image obtained using a SG-TC experiment. The tip starting position was 5  $\mu\text{m}$  above the chip surface (outside the channel), i.e., top left-hand corner of image. The substrate and tip potentials were 0.4 and 0.0 V, respectively. (C) SG-TC SECM image of the entire VACNF chip with conditions as (B).

maximum current could be detected, approximately aligning the electrodes at this separation. At this point, the image obtained was a projection of the diffusion of FcMeOH<sup>+</sup> over the time scale of the experiment as the gap between the electrodes was relatively large (several micrometers). The longer diffusion time yielded a magnified image compared to the real tip dimensions (Figure 4A). Thus, as  $d$  decreased, the gap and the diffusion time decreased, as shown by the smaller image of the substrate and the higher collection currents (Figure 4A). The  $z$  distance was decreased with smaller increments at this position and the process repeated until feedback current began, signaling a separation distance,  $d$ ,  $\sim 2$ – $3$  times the tip radius,  $a$ . At this position, a mirror image was obtained for the two electrodes (Figure 4C and D), and one can evaluate the gap between the two CNF tips according to the ratio between the feedback substrate current,  $i_{\text{subs}}$ , to the steady-state substrate current when the probe tip was far away,  $i_{\text{subs},\infty}$ . In this experiment,  $i_{\text{subs},\infty}$  was 55 pA (at  $E_{\text{subs}} = 0.35$  V vs Ag/AgCl, measured separately for  $\sim 1$ -mm gap) while  $i_{\text{subs}} = 530$  pA, and hence, the normalized ratio was  $I = 9.64$ . Interpolation of this value to the approach curves of Figure S1B yields the normalized distance (nanogap divided by radius) from which a nanogap of 4.4 nm is obtained using the experimental curve, and a nanogap of 15.8 nm is calculated by assuming the two electrodes possess a disk-shaped geometry. Note that the time needed for the FcMeOH<sup>+</sup> to diffuse across this gap was only 20–250 ns depending on the size of the gap.

**Vertically Aligned CNF Arrays.** Nanogap experiments were performed using VACNF arrays grown on a chip using conventional microfabrication technology.<sup>24</sup> Research into the construction of arrays of VACNFs such as these has increased substantially in recent years because of the potential application of such devices

in areas such as nanoelectronics and biosensors.<sup>29–31</sup> Modern methods for the growth of VACNFs can impart a high degree of control of the nanofiber location, height, diameter, shape, and orientation, enabling the construction of devices.<sup>32–34</sup> The chips employed in this study consist of 10 groups of addressable VACNFs, each group consisting of 4 CNFs. Applications of these devices may ultimately be found in areas such as electrochemical detection in microfluidic channels and probing the interior of biological cells. Moreover, these VACNF chips are very promising for SECM applications. In particular, they offer the possibility of forming a series of nanogaps by positioning a small SECM tip very close to the surface of the VACNFs as described here.

To locate the VACNFs within the channel, the SECM tip was first positioned  $\sim 500$   $\mu\text{m}$  above the exposed chip surface with the aid of a long-distance microscope. The electrochemical cell was then filled with FcMeOH solution, and an approach curve experiment was performed by applying 0.4 V to the SECM tip (to oxidize FcMeOH) and slowly moving the tip toward the chip. Using negative feedback control, the tip was positioned 5  $\mu\text{m}$  from the chip surface. At this point, the tip was outside the channel

- (29) Ren, Z. F.; Huang, Z. P.; Xu, J. W.; Wang, J. H.; Bush, P.; Siegal, M. P.; Provencio, P. N. *Science* **1998**, *282*, 1105.
- (30) Teo, K. B. K.; Hash, D. B.; Lacerda, R. G.; Rupesinghe, N. L.; Bell, M. S.; Dalal, S. H.; Bose, D.; Govindan, T. R.; Cruden, B. A.; Chhowalla, M.; Amaratunga, G. A. J.; Meyyappan, M.; Milne, W. I. *Nano. Lett.* **2004**, *4*, 921.
- (31) *Carbon Nanotubes: Science and Applications*; Meyyappan, M., Ed.; CRC Press: Boca Raton, FL, 2005.
- (32) Merkulov, V. I.; Hensley, D. K.; Melechko, A. V.; Guillorn, M. A.; Lowndes, D. H.; Simpson, M. L. *J. Phys. Chem. B* **2002**, *106*, 10570.
- (33) Moser, J.; Panepucci, R.; Huang, Z. P.; Li, W. Z.; Ren, Z. F.; Usheva, A.; Naughton, M. J. *J. Vac. Sci. Technol. B* **2003**, *21*, 1004.
- (34) Guillorn, M. A.; McKnight, T. E.; Melechko, A. V.; Austin, D. W.; Merkulov, V. I.; Simpson, M. L.; Lowndes, D. H. *J. Appl. Phys.* **2002**, *91*, 3824.

located at the center of the chip. This is demonstrated in Figure 5A, in which the SECM tip was scanned across a portion of the chip surface while the tip was in the negative feedback region. While located above the polymer coating of the chip, a lower tip current was observed due to hindered diffusion of FcMeOH, i.e., negative feedback. As the tip passed over the 20- $\mu\text{m}$ -wide channel, negative feedback decreased and the current increased. Therefore, feedback imaging could easily be used during these measurements to estimate the initial position of the tip, which is important to prevent tip crashes.

A SG-TC experiment was then performed to locate the VACNFs within the microfluidic channel. 0.4 V current was applied to the entire array of VACNFs to generate FcMeOH<sup>+</sup> and 0.0 V was applied to the SECM tip to reduce FcMeOH<sup>+</sup>. The tip was then scanned across the chip to locate the electroactive VACNFs, and an image obtained is shown in Figure 5B. As discussed previously,<sup>24</sup> these chips consist of addressable groups of four CNFs. The diffusion fields of closely spaced CNFs would overlap in this experiment, making it impossible to resolve a single CNF. The image shown in Figure 5B therefore cannot indicate whether the electroactive spot is due to a single CNF or a group of four. In either case, the diameter of the electroactive site estimated from Figure 5B (20  $\mu\text{m}$ ) is much greater than that expected for the VACNFs. This is due to diffusion of FcMeOH<sup>+</sup> away from the CNF over the time scale of the experiment.

Upon location of an electroactive spot in the chip, an SG-TC experiment was used to identify the positions of each group of CNFs within the chip. The resulting image is shown in Figure 5C. Eight electroactive sites are observed along the channel covering an  $x$  displacement of over 3 mm. Ten sites should be electroactive on these chips, and the two sites that are not seen in this image are to the left and right of those shown in Figure 5C. The shape of the SECM probe (0.5-cm taper, taper angle  $\sim 10^\circ$ ) caused the sides of the SECM tip to touch the inner sides of the channel before the tip was above the electroactive sites. Therefore, we were limited to imaging those eight sites in the center of the channel. Using the SG-TC imaging method described above, it was possible to locate and approach a single CNF within the channel. A series of images were recorded while decreasing the distance between the tip and the CNF in the channel (Supporting Information, Figure S2). The nanogap formed between the SECM tip and CNF substrate that was formed using this method was calculated to be 375 nm.

**Measurements of Homogeneous Kinetics in DMF at Nanogaps with Type G CNF Tips.** Type EPP CNF tips cannot be used in many nonaqueous solvents because the electrophoretic paint is not stable. However, nanogaps can be produced with two type G tips, even with larger tip radii (e.g., 10  $\mu\text{m}$ ), using the dual-electrode procedure described above. Here, the small substrate electrode was aligned vertically in the bottom of a Teflon electrochemical cell using a cylindrical Teflon tube to prevent any solution leakage by wrapping it with Teflon tape. This cell was filled, drop by drop, with 1 mM ferrocene (Fc) and 0.1 M tetra-*n*-butylammonium hexafluorophosphate (TBAPF<sub>6</sub>) in DMF and the level of solution checked frequently by performing LSV on the substrate electrode (Supporting Information, Figure S3a). When the solution just covered the electrode surface completely, a LSV with the maximum current was observed. In this situation,

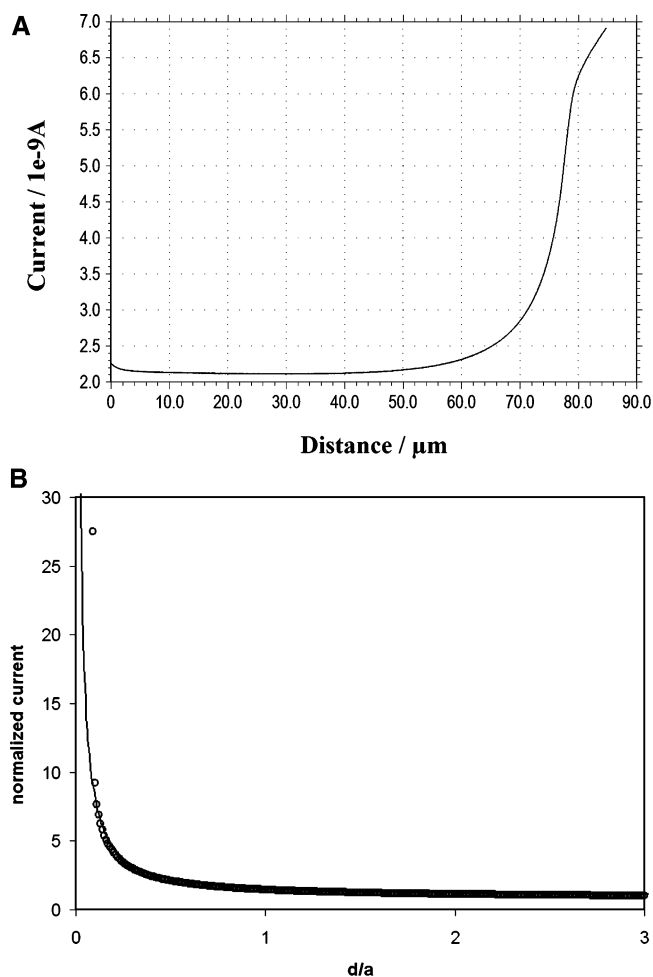


**Figure 6.** (A) Approach curve for a 10- $\mu\text{m}$  CNF electrode over a similar-sized one when the electrodes were not completely perpendicular. The potential of the tip and substrate electrodes were 0.9 and 0.4 V vs Ag QRE, and the scan rate was 0.5  $\mu\text{m}/\text{s}$ . (B) Approach curve under the same conditions as (A) but after changing the tilt compensation using the screws on the SECM cell stage.

the solution over the substrate electrode was  $\sim 5\text{--}10$   $\mu\text{m}$  thick (Supporting Information, Figure S3b). Then the probe tip was held at 0.8 V versus Ag QRE (a sufficiently positive potential to oxidize Fc) and the SECM tip approached from the air to the air/DMF solution interface above the substrate electrode. When the tip contacted the solution surface, the current increased dramatically and the tip was stopped when the tip current increased above the level of the instrument offset current found in the air,  $\sim 100\text{--}200$  pA. This placed the probe tip a few micrometers above the substrate electrode. To form the nanogap, the procedure described earlier was used to focus on and obtain a good image of the substrate (Supporting Information, Figure S4). The tip was then located over the substrate electrode (Supporting Information, Figure S3c) and an approach curve could be obtained. If the approach curve suggested that the tip and substrate electrode were not perpendicular (Figure 6A) and the electrodes passed one another as the  $z$  piezo was advanced, the plane of the substrate electrode disk had to be adjusted. This was accomplished by scanning the tip very close to the substrate surface in both  $x$  and  $y$  directions at a slow scan rate and monitoring the tip current as a function of position. The leveling screws on the SECM cell stage

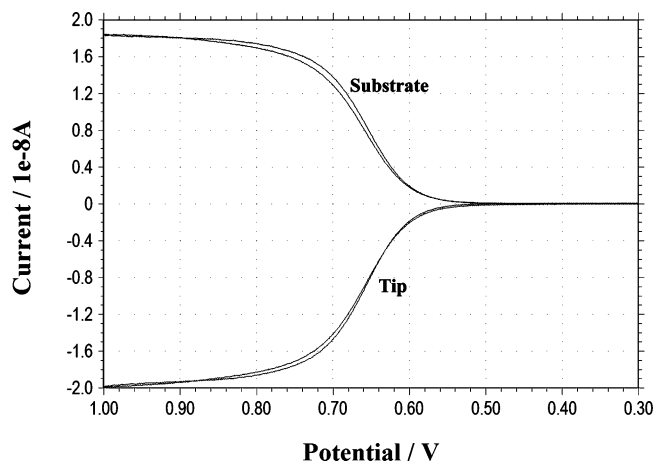


**Figure 7.** Cyclic voltammogram of 1 mM ferrocene and 0.1 M TBAPF<sub>6</sub> in DMF at a 10- $\mu$ m CNF electrode located 100 nm over a similar-sized electrode held at 0.4 V vs Ag QRE and collection current at the substrate electrode vs the tip potential.

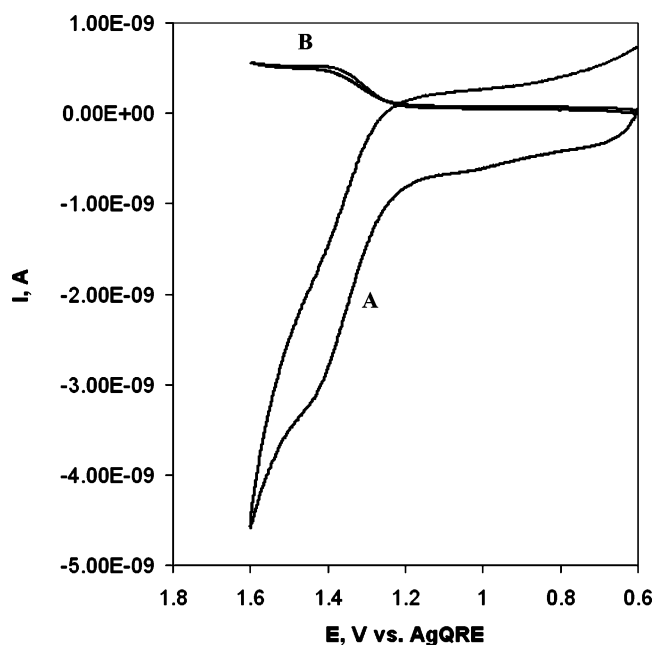


**Figure 8.** Cyclic voltammograms for the oxidation of 2 mM guanosine in DMF/0.1 M TBAPF<sub>6</sub> obtained at the tip (A) and substrate (B) electrodes.  $E_s = 1.0$  V vs Ag QRE. The tip potential sweep rate was 20 mV/s. The distance between the tip and the substrate was  $\sim$ 100 nm.

were adjusted until the tip current remained constant as the tip scanned over the substrate surface in both the  $x$  and  $y$  directions. We could then relocate the tip over the substrate electrode and obtain an approach curve with good feedback (Figure 6B). Images taken under these conditions show regeneration of ferrocene on the surface of the substrate electrode causing an enhanced current at both electrodes (Supporting Information, Figure S4).

When the electrodes were well aligned, one can measure the distance between the two electrodes by very slowly moving the tip toward the substrate until it just touched the substrate electrode to get the  $L = 0$  point. The tip was then moved back for a known distance, e.g., 100 nm, and an approach curve taken. Cyclic voltammograms with a 10- $\mu$ m CF tip located 100 nm over a similar

sized electrode used as the substrate (held at a constant potential 0.4 V vs Ag QRE) and the collection current at the substrate electrode versus the tip potential are shown in Figure 7. This type of nanogap is useful in the detection of an unstable tip generated species and measurements of fast homogeneous kinetics.<sup>13</sup> An example is the detection of the guanosine radical cation, Gs<sup>+</sup>, as shown in Figure 8, where Gs<sup>+</sup> generated at a constant potential on the substrate in dry DMF/0.1 M TBAPF<sub>6</sub> can be collected on the surface of the probe tip. Details of this experiment will be published elsewhere.

## CONCLUSIONS

We have demonstrated that carbon fibers can be flame-etched and insulated to yield nanometer-size tips suitable for SECM measurements. The approach curve of CNF tips over a Pt conductive disk supports feedback currents that correspond to a gap of less than 10 nm. In a complementary experiment, an electrochemical recognition of one CNF tip by another was performed employing the SG-TC mode of the SECM. During feedback, a mirror image of the two tips was obtained and from the measured currents we detected a nanogap of less than 16 nm between the two nanoelectrodes. This novel method is interesting for investigations of short-lived intermediates that can be simultaneously electrogenerated at one electrode and detected at the other. These tips have also been used to image arrays of vertically aligned carbon nanofibers.

## ACKNOWLEDGMENT

This work has been supported by a grant from the National Science Foundation (CHE 0451494). The authors thank T. E. McKnight, A. V. Melechko, and M. L. Simpson of the Oak Ridge National Laboratory for providing the arrays of vertically aligned carbon nanofibers. These devices were supported in part by the National Institute for Biomedical Imaging and Bioengineering under assignment 1-R01EB000433-01, and through support from the Material Sciences and Engineering Division Program of the DOE Office of Science. A portion of their fabrication was conducted at the Center for Nanophase Materials Sciences, which is sponsored at Oak Ridge National Laboratory by the Division of Scientific User Facilities, U.S. Department of Energy. R.T.-V. thanks the Israel Science Foundation and the Technion–Israel Institute of Technology for a postdoctoral fellowship. M.A.M. thanks the Iranian Ministry of Science, Research and Technology for a visiting scholarship.

## SUPPORTING INFORMATION AVAILABLE

Type EPP electrode approach curves, a schematic representation of locating the tip electrode over the substrate electrode, a description of the method used to locate single CNFs within the array of VACNFs and the resulting SECM images are available free of charge via the Internet at <http://pubs.acs.org>.

Received for review April 17, 2006. Accepted August 1, 2006.

AC060723M